 doi:10.20944/preprints202107.0327.v2

Article

Modeling the Dual-Function Effects of Free Radical and Cationic Hybrid-Photopolymerization in Iodonium/Amine System

Jui-Teng Lin[1,*] and Kuo-Ti Chen[2]

[1] Medical Photon Inc., 10F, No. 55, Sect.3, Xinbei Blvd, Xinzhuang, New Taipei City, Taiwan; jtlin55@gmail.com
[2] School of Life Science, National Taiwan Normal University, Taipei, Taiwan; tony022199@msn.com
* Correspondences: jtlin55@gmail.com

Abstract: The synergistic features of a three-component, photoinitiating system (A/B/C) based on the measured data and proposed mechanism of Liu et al. are analyzed. The co-initiators/additives B and C have dual-functions of : (i) regeneration of photoinitiator A, and (ii) generation of extra radicals for enhanced conversion efficacy (CE). The synergistic effects led to higher CE for both free radical polymerization (FRP) and cationic polymerization (CP). The CE of FRP has 3 terms due to the direct (tyep-I) coupling of the triplet state of A with the monomer (M) and the coupling of the two radicals, R and R', with M. The CE of CP has a transient state proportional to the effective absorption constant (b), the light intensity (I) and initiator concentration (A_0), but a steady state is independent of the light intensity (I). For the CE of FRP, the contribution from radical R had two cases: (i) linear dependence on $T=bIA_0$, or (ii) nonlinear square root dependence $T^{0.5}$. The synergistic effects led to higher conversion of FRP and CP, consistent with the measured results. The theoretically predicted new features include: (i) co-initiator [C] which always enhances both FRP and CP conversions, and (ii) co-initiator [B] which leads to more efficient FRP, but it also reduces CP.

Keywords: polymerization kinetics; photoinitiator; monomer conversion profile; synergistic effects

1. Introduction

Compared to the conventional thermal-initiated polymerization, there are several advantages for photopolymerization, including fast and controllable reaction rates and spatial and temporal control over the formation of the material, without the need for high temperatures or harsh conditions [1]. Photopolymerizations using various light with wavelengths in the UV, visible and near IR have been studied for both industrial and medical applications. A variety of photoresponsive materials, such as conjugated polymers, have been reported for additive manufacturing (AM) and recently for 3D and 4 D bioprinting [3,4]. For 3D photo printings the key factors include polymerization depth, resolution precision and speed, in which the monomer conversion efficacy could be improved by various strategies. The reported conversion enhancing methods include the use of novel materials as enhancers or co-initiators in both single and multiple components [5-8]. Experimental two stage polymerization under two wavelengths to eliminate the oxygen inhibition effects has also been reported [9-11]. Sequential network formation has also been achieved with many different types of polymerization materials, such as thiol–Michael/acrylate hybrid, epoxy/acrylate curable resins, thiol–acrylate/thiol–acetoacetate thermosets, and thiol–ene/epoxy-based polymers [12-14].

UV light (at 365 nm) has been commonly used in most type-I photoinitiators (PI) for the photopolymerization of (meth)acrylate monomers [1-3]. However, the UV wavelength suffers the disadvantages of being unsafe to skin and eyes, small penetration depth and larger light scattering in tissues [1]. Camphorquinone (CQ), due to its good visible light absorption properties, is the most common type-II PI for the polymerization of (meth)acrylates under visible light [15,16].

 doi:10.20944/preprints202107.0327.v2

Various strategies to reduce oxygen inhibition of photoinduced polymerization have been proposed, such as using co-initiators or addition of oxygen scavengers, and the thiol-ene and thiol-acrylate-Michael systems which are insensitive to oxygen [8,9]. Dual-wavelength (red and UV) photopolymerization has also been reported, in which pre-irradiation by the red light eliminated the oxygen inhibition effect and thus enhanced the conversion efficacy of the UV light [10].

The classical diaryliodonium salts, such as diaryliodonium, suffer low solubility in monomers and when used as a photopolymerization initiator results in formation of side products due to the release of HF. To overcome this drawback, Kirschner et al. [15] recently reported a new counter anion-free and fluoride-free aryliodonium ylides (AY) to avoid the formation of HF and to enhance their solubility. They reported (CQ)/amine/AY as a new and efficient PI system for the polymerization of methacrylates under air and blue light (477 nm) irradiation, resulting in additional reactions and initiating radicals for improved conversion efficacy.

Various strategies for enhanced conversion have been reported, including the use of multiple light wavelength [9-11, 20-21], and co-initiators systems [12-14, 23] An example of a dual-wavelength (UV 365 nm and blue 470 nm) system for enhanced conversion by reducing the oxygen inhibition was reported by de Beer et al. [8,9] for the photopolymerization of methacrylate formulated with camphorquinone (CQ) and ethyl 4-(dimethylamino)benzoate (EDAB), where the CQ was the blue-light active initiator (A), butyl nitrite (BN) was the UV-activated initiator (B), and EDAB was a co-initiator (or donor D). The photochemical decomposition of BN results in the formation of nitric oxide (N), an efficient inhibitor of radical-mediated polymerizations, and alkoxide radicals (X) for extra polymerization initiation, besides the initiation radicals (R) generated by the blue-light

An example of a 2-wavelength (red and UV) system (without the blue-light) for 3D printing was reported by Childress et al. [10], in which a monomer of di(ethylene glycol) ethyl ether acrylate (DEGEEA) mixed with zinc 2,9,16,23-tetra-tert-butyl-29H,31H-phthalocyanine (ZnTTP) as an initiator under a UV-light, for which the ZnTTP/DEGEEA has distinct absorption peaks at UV-365 nm and red-635 nm, respectively, and thus it can be independently excited by a UV and a red light, respectively. Our group [19] reported the theoretical modeling for a 2-wavelength system reported by Childress et al. [10]. The novel strategy, using 3–wavelengths of uv, blue and red lights was recently proposed by our group [21] theoretically for future experimental studies.

Various enhancing strategies for photopolymerization have been reported by us and others, including one component (or monomer) and one-wavelength [15-18,22], two-components and one wavelength 12,14], two wavelengths [9-11,19,20), three-wavelengths [21] and three-components, one-wavelength systems [13,23]. We note that all these systems have been theoretically and experimentally studied, except the 3–wavelength systems which we recently proposed theoretically [21]. The synergistic effects leading to higher monomer conversion can be achieved by co-initiators, additional radicals and multiple wavelengths for reduced oxygen-inhibition. Greater details of synergistic effects may be found in a Review article by us [24].

This article will present, for the first time, the kinetics of the synergistic features of the 3-initiator, [A], [B] and [C], system based on the measured data and proposed mechanism of Liu et al. [22], The co-initiator [B] and [C] have dual functions of: (i) regeneration of initiator [A]; and (ii) generation of extra radicals. The synergistic effects led to higher conversion for FRP and CP. The key factors and rate constants influencing the conversion efficacy were explored by analytic formulas of the conversion rate functions, derived from a kinetic model for a 3-initiator and 2-monomer system. While certain features predicted in this article are consistent with the measured data of Liu et al. [22], some new, theoretically predicted findings are explored for future experimental studies.

2. Methods and Modeling Systems

2.1. Photochemical Kinetics

Preprints (www.preprints.org) | NOT PEER-REVIEWED | Posted: 2 June 2022 doi:10.20944/preprints202107.0327.v2

Figure 1 shows a 3-initiator system (A/B/C), in which the ground state of initiator-[A] was excited to its first-excited state PI*, and a triplet excited state T. The triplet state T interacts with initiators [A] and [B] to produce radicals R, R' and R"; and interacts with co-initiator [C] to produce radical S'and S; in which the coupling of the radicals R" with [C] and S' with [B] lead to the regeneration of [A]. Radicals R and S lead to the free radical polymerization (FRP), and radical S' leads to cationic polymerization (CP), via monomers M and M', respectively. For a system with [A] alone, T, R' and R could be responsible for FRP. In general, the terminations of our proposed scheme include the couplings of R+R (bimolecule), R+R', R+S', and S+S, in the two monomers system (M + M'), in which (T,R,S) + M is for FRP and S'+M' is for CP. We will show later that Fig. 1 is more general than the proposed Scheme of Liu et al. [22].

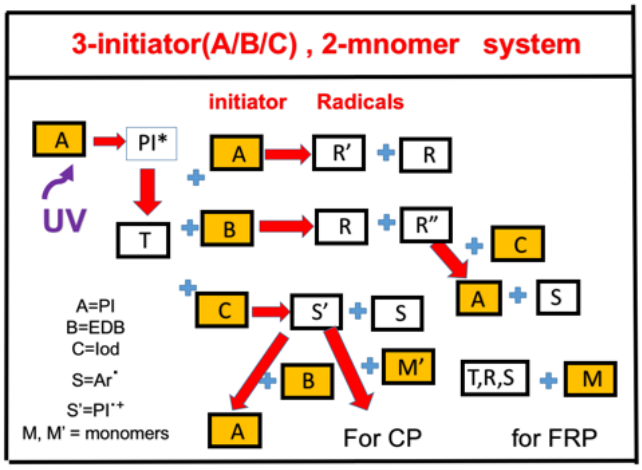

Figure 1. Schematics of a 3-initiator system, (A/B/C), where [A] is the ground state initiator, having a first excited state PI*, and a triplet state T, which interacts with initiator [A] and [B] to produce radical R; and interacts with initiator [C] to produce radical S, in which the coupling of the radical R" with [C] and S'with [B] both lead to the regeneration of [A].

A specific system reported by Liu et al. [22] corresponds to the mechanism of Fig. 1, where [A] is benzophenone (BP) photoinitiator, co-initiator [B] is ethyl 4-(dimethylamino)benzoate (EDB), and [C] is (4-*tert*-butylphenyl)iodonium hexafluorophosphate (Iod). As shown in Scheme 1, under a UV (365 nm) LED irradiation, [A] transformed from its ground state (PI) to an excited triple state ^{1,3}PI (shown by r1 of Scheme 1), which couples with PI to produce radicals PI-H^{o} (or R) and PI(-H)^{o} (or R') (shown by r2). In the presence of EDB, extra radical EDB(-H)^{o} (or R) and PI-H^{o} (or R") were produced (shown by r3). T could couple with [C] to produce the aryl radical, Ar^{o}, and PI^{o+} (shown by r4), where radicals Ar^{o} (or S) and EDB(-H)^{o} (or R) lead to FRP and PI^{o+} (or S') leads to CP. Furthermore, PI-H^{o} (or R") could couple with Iod (or C) to produce extra radical Ar^{o} for FRP (shown by r5) and also regenerate PI (or [A]). Radical PI^{o+} (or S') could couple with EDB to regenerate PI (or [A]), shown by r6. Associated with the photolysis of BPC1/Iod and BPC1/EDB/Iod, the photoredox catalytic cycle was proposed in the three-component PI/EDB/Iod system (shown by r5 and r6). The regeneration of PI sped up the photopolymerization and slowed down the consumption of PI in the photolysis experiments. Trimethylolpropane triacrylate (TMPTA) and (3,4- epoxycyclohexane)methyl 3,4-epoxycyclohexylcarboxylate (EPOX) were used in our prior work as benchmark monomers for FRP and CP, respectively.

However, we note that our Fig. 1 here is more general than the Scheme proposed by Liu et al. [22] which ignored the termination scheme due to the couplings of R+R (bimolecular), R+S, and R+S'. Furthermore, the measured data of Liu et al. [22] for the case of CP was limited to the two initiators, of [A] and [C], although 3-initiator systems of [A]/[B]/[C] were studied in FRP. Our modeled system of Fig. 1 and the associated kinetic equations to be shown later include 3-initiator for both FRP and CP. The mechanism of a 3–initiator

Preprints (www.preprints.org) | NOT PEER-REVIEWED | Posted: 2 June 2022 doi:10.20944/preprints202107.0327.v2

and 2-monomer, A/B/C/M/M'system proposed by Liu et al. [22] is shown in the following schematic equations of (r1) to (r6).

$$PI \xrightarrow{h\nu} {}^{1,3}PI \quad (r1)$$

$${}^{1,3}PI + PI \longrightarrow PI^{\bullet -} + PI^{\bullet +} \longrightarrow PI\text{-}H^{\bullet} + PI_{(-H)}^{\bullet} \quad (r2)$$

$${}^{1,3}PI + EDB \longrightarrow PI^{\bullet -} + EDB^{\bullet +} \longrightarrow PI\text{-}H^{\bullet} + EDB_{(-H)}^{\bullet} \quad (r3)$$

$${}^{1,3}PI + Ar_2I^{+} \longrightarrow PI^{\bullet +} + Ar_2I^{\bullet} \longrightarrow PI^{\bullet +} + Ar^{\bullet} + ArI \quad (r4)$$

$$PI\text{-}H^{\bullet} + Ar_2I^{+} \longrightarrow PI + Ar^{\bullet} + ArI + H^{+} \quad (r5)$$

$$PI^{\bullet +} + EDB \longrightarrow PI + EDB^{\bullet +} \quad (r6)$$

Scheme 1. The proposed chemical reactions of a PI/EDB/Amine 3-component system for a hybrid FRP and CP system with two monomers, TMPTA and EPOX (not shown in Scheme 1, see text) [22].

Based on Scheme 1, the initiator concentration, [A], [B] and [C], and the monomers convertion kinetics of M (for FRP) and M'(for CP) are given by: (detailed derivations are shown in the Apendix). We note that dM/dt presents the time derivative of M in time (t). T, S, R and S' are the short hand notations for the concentrations of the triplet state, radical S, R, and S', respectively; and k, K, k', and K' are the associate coupling constants (referred to Fig. 1 and Apendix for more details).

$$\frac{dM}{dt} = -(kT + KS + k'R)M \quad (1)$$

$$\frac{dM'}{dt} = -K'S'M' \quad (2)$$

Eq. (1) shows that FRP was due to 3 contributions: from the direct (type-I) coupling kTM term and the radical S and radical R, whereas CP had only one contribution from the catonic radical S', shown in Eq. (2). Numerical simulation is, in general, required for the solution of M and M', due to the inter-couplings of the radicals (R,S, S') and additives, [A], [B] and [[C]. We will focus on the synergistic effects based on the analytic formulas, derived in the Appendix.

The steady state concentration of radical R, as given by the Appendix, Eq. (A11), is given by the solution of Eq. (3)

$$k'R^2 + GR - P = 0 \quad (3)$$

where G=k"S+k'M, and P= (k_1[A]+k_2[B]).

Solving for R, we obtain

$$R = 0.5(-G + \sqrt{G^2 + 4k'H}\,)/k' \quad (4)$$

Analytic formulas of R were obtained for two special cases as follows.

Case (i), for unimolecular termination dominant, or G>>k'P, we obtained R= P/G, which is a linear increasing function of (k_1[A]+k_2[B])T/(k"S+k'M).

Case (ii), for bimolecular termination dominant, with P>> GR, we obtained R=[P/k']$^{0.5}$. a nonlinear function of a square root function, [(k_1[A]+k_2[B])T/k']$^{0.5}$.

3.. Results and discussion

3.1 Formulas for conversion efficacy (CE)

Preprints (www.preprints.org) | NOT PEER-REVIEWED | Posted: 2 June 2022 doi:10.20944/preprints202107.0327.v2

The CE of CP, defined by CE'=1-M'/M_0', which is the time integral of Eq. (2), we obtain , from Eq. (A13) of the Appendix,

$$CE'=[1- k_7B_0/(K'M_0')]K'D(bIC_0A_0)H(t), \quad (5)$$

with H(t)=[1- exp(-d't)]/d', with a revised d'=$k_3T'/(kM_0)$+X', for a non-constant [A]= A_0 exp(-X't). It shows that, in the presence of [B], the CP is reduced by a reduction factor of F'= [1- $k_7B_0/(K'M_0')$]. The CE' has a transient state proportional to bIt(C_0A_0), but a steady state given by TE'=K'D(bIC_0A_0)/d'= K'D(C_0A_0)[$k_3/(kM_0)$], which is independent of the light intensity (I).

The CE of FRP defined by TE=1-M/M_0, the solution of Eq. (1), is much more complex than CE of CP. From Eq. (A14) of the Appendix, including the revised factor for T', we obtain

$$CE= (T''/M_0)t+KD'H(t)+ KD''H'(t) + P'H''(t) , \quad (6)$$

where a revised T' is T''=(bIA_0)[1- exp(-X't)]/X'. The above CE has 3 terms: (i) from the direct coupling of T and M; (ii) coupling of radical S and M, and (iii) coupling of radical R and M, the terms of KD'H', KD'''H'' and P'H'''. For case (i) linear case, we obtain H''(t)= Pt+P'H'''(t), with H'''=[1- exp(d''t)]/d'', with P= $k_1(A_0^2/M_0)T'$, , P'=$k_2(B_0/M_0)T'$, and d''= [$k_2T'/(kM_0)$+ $0.5k_7k_3T't[C_0/(kM_0K'M_0')$]t. For case (ii) nonlinear square root case, k'R=[$k'(k_1[A]+k_2[B])T]^{0.5}$, we obtain H''(t)= Vt+V'H'''(t), with V= $(k_1 (A_0M_0)T')^{0.5}$, , V'=$(k_2 (B_0M_0)T')^{0.5}$. Therefore Eq. (6) shows that CE is proportional to T and $T^{0.5}$, for case (i) and (ii), respectively.

3.2 *Synergistic effects*

As shown by Fig. 1, and Eqs. (1) to (6), the following synergistic features of the 3-initiator system A/B/C can be summarized as follows.

(a) Co-initiator [B] has multiple functions of : (i) regeneration of initiator [A] leading to higher FRP conversion; (ii) producing of extra radical R and radical R''; and (iii) coupling of R'' with [C] leads to radical S, in which both R and S lead to FRP.

(b) Similarly, co-initiator [C] has functions of : (i) regeneration of initiator [A] via the coupling of S' and [B], leading to higher FRP conversion; (ii) generation of cationic radical S′ for CP conversion; and (iii) enhancing FRP by producing radical S (as shown by Figure 1).

(c) As shown by Eq. (5) and (6) the CE of FRP has 3 contributions, kTM, KSM and k'R. Therefore it is always higher than that of CP having only one contribution, K'S'M', which is comparable to KSM.

(d) The presence of [C] always leads to higher FRP via the extra radical S and the regeneration of [A]. However, the presence of [B] consumes radical S', and hence reduces the FRP. Therefore the net enhanced effects of [C] on FRP is governed by the relative strength of regeneration of [A] and the reduction effect, as shown by our formula in Eq. (5) with a reduction factor F'= [1- $k_7B_0/(K'M_0')$]. These non-common features were not explored by Liu et al. [22], and they could not be easily predicted without the detailed mathematical efforts derived here.

(e) From Eq. (5), the CE of CP has a transient state proportional to bIt(C_0A_0), but a steady state given independent of the light intensity (I).

(f) From Eq. (6) for the CE of FRP, the contribution from radical R could have two cases: (i) linear dependence proportional to T=bIA_0, or (ii) nonlinear square root dependence proportional to $T^{0.5}$. However, the contribution from radical S has a linear dependence of T'=bIA_0, The nonlinear feature is due to the bimolecular termination included in the coupling term of $k'R^2$ in Eq. (A5).

(g) For a very weak type-I coupling (or $k_1[A]<< 1/g$, or type-II dominant, we obtain d[A]/dt=0, which defines a perfect regeneration with [A]=A_0, a constant. In non-perfect regeneration, [A]= A_0 exp(-X't), and the depletion of [A] leads to a lower conversion and

Preprints (www.preprints.org) | NOT PEER-REVIEWED | Posted: 2 June 2022 doi:10.20944/preprints202107.0327.v2

a time-dependent light intensity deviating from the conventional Beer-Lambert law, given by $I(z,t)=I_0 \exp(-b'[A]z)$. Greater details can be found by our previous work [25].

The above theoretically predicted new findings for synergistic effects were not explored in the measured work of Liu et al. [22]. Greater details may be found in our Review article [24].

Figure 2 shows the results based on Eq. (5) for CP conversion re-expressed as $CE'=Q[1-\exp(-d't)]$, with $Q=[1- k_7B_0/(K'M_0')]K'D(bIC_0A_0)$, for various values of Q and the initiator depletion rate d'. We note that larger Q results in a higher steady-state profile, as shown by Fig. 2(A). Furthermore, the profile rising rates are given by d (proportional to bIA_0). Higher light intensity (I), larger initiator concentration, or stronger absorption (b) leads to a faster depeltion of [A] and hence faster rising of the conversion profile, shown by Figure 2(B). We note that for the same Q value, the CP conversion profiles having different d'-values (or bIg) reach the same steady state. However, we have previously reported different features of FRP [24] that larger d' value reaches a lower steady state conversion (not shown in this article), which is fundamentally different for FRP and CP profiles. The above theoretically predicted new findings are not explored in the measured work of Liu et al. [22].

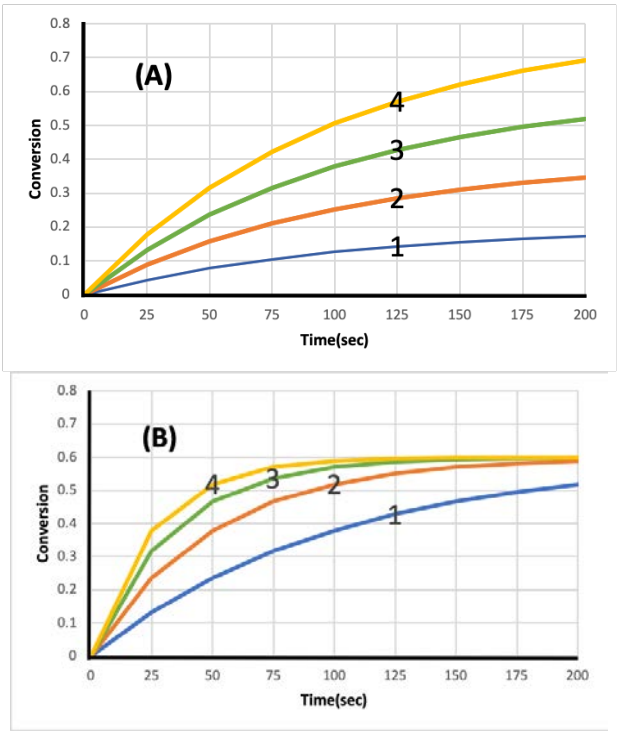

Figure 2. The calculated CP conversion profiles for various Q and d' values: (A) for fixed d'=0.01, and Q= (0.2, 0.4,0.6, 0.8), for Curves 1, 2, 3 and 4; and (B) for fixed Q=0.6, and d'= bIg=(0.01, 0.02, 0.03, 0.04) for Curves 1, 2, 3 and 4, respectively.

3.2. Analysis of measured results

Besides the synergistic effects described in last section, our formulas shown by Eqs. (18) to (23), may be used to analyze the measured results of Liu et al. [22] as follows:

Figure 3 in Ref. [22] for the cationic polymerization of EPOX showed that the BPC1/Iod system had the highest conversion (44%) due to its highest light absorption. The role of light absorption was shown by Eq. (A9) and (A10), in which the conversion rate is an increasing function of b, defined by $b=83.6a'wq$, where a' is the molar extinction coefficient, w is the UV light wavelength and q is the triplet state quantum yield. BPC1-

 doi:10.20944/preprints202107.0327.v2

BPC4 have higher molar extinction coefficients than that of C5-C8; therefore the CP conversion rates of EPOX for the BPC1-BPC4/Iod systems are faster than C5-C8/Iod systems for the same initial concentration of PI and Iod. Fig. 3 of Liu et al. [22] may be compared with our Fig.2(A)here, where a higher Q value leads to larger steady-state conversion, as also shown by Eqs. (5) and (6).

Figure 4b in Ref. [22] showed that a higher FRP conversion of TMPTA in the presence of PI/EDB systems compared to that of the PI alone, shown by Fig. 4a. This enhanced polymerization is due to the increase of the conversion rate as shown by the additional term $k_2[B]$ of Eq. (20). EDB (or co initiator [B]), as a H donor, has an effective interaction with PI to generate radicals which promote the free radical polymerization, so the PI/EDB systems have better polymerization performance than the PI alone systems. Figure 4d of Ref. [22] showed that the FRP conversion of TMPTA initiated by PI/EDB/Iod (or A/B/C) systems was better than that by the PI/EDB (or A/B) and PI/Iod (or A/C) systems. This can be easily realized by our Eq. (1), that the conversion rate is an increasing function of kT+KS+k'R. That is, a 3-initiator system is more efficient than that of two (with [B] or [C]=0) and one initiator (with [B]=[C]=0) systems. In the PI/EDB/Iod system, the triple state (T) reacts with PI, EDB and Iod at the same time. There is a photoredox catalytic cycle in the 3-initiator system and the regeneration of PI speeds up the polymerization, in additional to the free radicals (R, S and S'). Therefore, the PI/EDB/Iod systems have better polymerization performances than the PI/EDB and PI/Iod systems.

Figure 5 of Ref. [22] showed that the consumption rate of BPC1 in the BPC1/TEOA/Iod system was slower than in the BPC1/Iod system. The photoredox catalytic cycle in the three-component system could regenerate BPC1, as shown by Eq. (1) and (8). Figure 6 and S1 of Ref. [22] showed that the consumption rates of BPC1-BPC4 were faster than C5 and C7 due to the presence of the benzophenone moieties in the BPC1-BPC4 structures which promoted the reaction between PI and amine. The photolysis demonstrated the benzophenone-carbazole PIs had high reactivity. Higher reactivity of co-initiator benzophenone led to higher conversion, as shown by our Eq. (5) and (6) here.

Figure 7 of Ref. [22] showed the fluorescent properties as evidence of the interaction capacity of the PIs with the additives in the excited singlet state. The role of triple-state quantum yield (q) was also shown by the b factor of Eqs. (20) and (21). The fluorescence experiments demonstrated that the benzophenone-carbazole PIs could be quenched easily by additives. The high electron transfer quantum yields showed that electron transfer occurred effectively between the benzophenone-carbazole PIs and EDB/Iod and therefore, led to high polymerization conversions. These features are also predicted by our Eq. (5) and (6) here.

5. Conclusions

This article presents, for the first time, the kinetics of the synergistic features of a 3-initiator, [A], [B] and [C], system based on the measured data and proposed mechanism of Liu et al. [22]. The co-initiators [B] and [C] have dual functions of: (i) regeneration of initiator [A]; and (ii) generation of extra radicals. The synergistic effects led to higher conversions for FRP and CP. These features were also shown by the measured work of Liu et al. [22]. However, there are other theoretically predicted new features (findings) in this article, which were either not identified or explored by Liu et al. [22], including the following lists.

(i) Co-initiator [C] always enhances both the FRP and CP conversions, whereas co-initiator [B] leads to a more efficient FRP, but it also consumes [C] and thus reduces CP conversion.

(ii) The contribution of radical R for FRP could have two cases: (a) the linear case of R on $T'=bIA_0$, or (b) the nonlinear square root dependence $T^{0.5}$. However, the contribution from radical S has a linear dependence of $T'=bIA_0$, The nonlinear feature is due to the bimolecular termination of radical R.

(iii) The steady state conversion profile of CP , as shown by Fig. 2 (B), reaches a constant and is independent of the light intensity, whereas higher light intensity caused a lower steady state value for the profile of FRP.

Acknowledgments: JTL thanks an internal grant of Medical Photon Inc. and the computer drawings by Jonathan Y.K. Hu (Kaohsiung American School, Taiwan) and

Potential Conflicts of Interest: Jui-Teng Lin is the CEO of Medical Photon Inc.

References

1. Fouassier, J. P. & Lalevée, J. Photoinitiators for Polymer Synthesis-Scope, Reactivity and Efficiency. Wiley-VCH Verlag GmbH & Co. KGaA: Weinheim, 2012.
2. Yagci, Y., Jockusch, S. & Turro, N.J. Photoinitiated polymerization: Advances, challenges and opportunities. *Macromolecules* **43**, 6245–6260 (2010). doi.org/10.1021/ma1007545.
3. Ligon, S.C.; Liska, R.; Stampfl, J.; Gurr, M.; Mulhaupt, R. Polymers for 3D printing and customized additive manufacturing. *Chem. Rev.* **2017**, *117*, 10212−10290. doi.org/10.1021/acs.chemrev.7b00074.
4. Takagishi, K.; Umezu, S. Development of the improving process for the 3D printed structure. *Sci. Rep*. **2017**, *7*, 39852. doi.org/10.1038/srep39852.
5. Shusteff, M.; Browar, A.E.M.; Kelly, B.E.; Henriksson, J.; Weisgraber, T.H.; Panas, R.M.; Fang, N.X.; Spadaccini, C.M. One-step Volumetric Additive Manufacturing of Complex Polymer Structures. *Sci. Adv.* **2017**, *3*, 7. doi.org/10.1073/pnas.1605271113.
6. Janusziewicz, R.; Tumbleston, J.R.; Quintanilla, A.L.; Mecham, S.J.; DeSimone, J.M. Layerless Fabrication with Continuous Liquid Interface Production. *Proc. Natl. Acad. Sci. USA* **2016**, *113*, 11703−11708. //doi.org/10.1073/pnas.1605271113.
7. Kelly, B.E.; Bhattacharya, I.; Heidari, H.; Shusteff, M.; Spadaccini, C.M.; Taylor, H.K. Volumetric Additive Manufacturing via Tomographic Reconstruction. *Science* **2019**, *363*, 1075−1079. DOI: 10.1126/science.aau7114
8. de Beer, M.P.; van der Laan, H.L.; Cole, M.A.; Whelan, R.J.; Burns, M.A.; Scott, T.F. Rapid, Continuous Additive Manufacturing by Volumetric Polymerization Inhibition Patterning. *Sci. Adv.* **2019**, *5*, 8. DOI: 10.1126/sciadv.aau8723.
9. van der Laan, H.L.; Burns, M.A.; Scott, T.F. Volumetric Photopolymerization Confinement through Dual-Wavelength Photoinitiation and Photoinhibition. *ACS Macro Lett.* **2019**, *8*, 899–904. doi.org/10.1021/acsmacrolett.9b00412.
10. Childress, K.K., Kim, K., Glugla, D.J., Musgrave, C.B., Bowman, C.N. & Stansbury, J.W. Independent control of singlet oxygen and radical generation via irradiation of a two-color photosensitive molecule. Macromolecules **52**(13):4968–4978 (2019). doi.org/10.1021/acs.macromol.9b00424.
11. Scott, T.F.; Kowalski, B.A.; Sullivan, A.C.; Bowman, C.N.; McLeod, R.R. Two-Color Single-Photon Photoinitiation and Photoinhibition for Subdiffraction Photolithography. *Science* **2009**, *324*, 913−917. DOI: 10.1126/science.1167610
12. Claudino,M.; Zhang,X.; Alim,M.D.; Podgórski,M.; Bowman, C. N. Mechanistic Kinetic Modeling of Thiol-Michael Addition Photopolymerizations via Photocaged "superbase" Generators: An Analytical Approach. Macromolecules 2016, 49, 8061−8074. DOI:10.1021/acs.macromol.6b01605
13. Huang, S.; Sinha, J.; Podgorski, M.; Zhang, X.; Claudino M. Bowman, C.N. Mechanistic modeling of the Thiol−Michael addition polymerization kinetics: Structural effects of the Thiol and Vinyl monomers. *Macromolecules* **2018**, *51*, 5979–5988. https://doi.org/10.1021/acs.macromol.8b01264
14. Chen, K.T.; Cheng, D.C.; Lin, J.T.; Liu, H.W. Thiol-Ene photopolymerization in thick polymers: kinetics and analytic formulas for the efficacy and crosslink depth. *Polymers* **11**, 1640 (2019) doi:10.3390/polym11101640.
15. Kirschner, J.; Paillard, J.; Bouzrati-Zerell, M.; Bechi J.M.; Chelli S; Lakhdar, S.;Lalevee, J. Aryliodonium ylides as novel and efficient additives for radical chemistry: example in camphorquinone (CQ)/Amine based photoinitiating systems. *Molecules* **24**, 2913 (2019); doi:10.3390/molecules24162913.
16. Wertheimer CM,; Elhardt C, ; Kaminsky SM,; Pham L.; Pei Q.; Mendes, B.; Afshar S; Kochevar J.E. Enhancing rose Bengal photosensitized protein crosslinking in the cornea. Invest. Ophthalmol Vis Sci. 2019, 60, 1845-1852. DOI: 10.1167/iovs.19-26604.

17. Schmitz C,; Halbhuber A,; Keil D,; Strehmel, B. NIR-sensitized photoinitiated radical polymerization and proton generation with cyanines and LED arrays. Prog. Org. Coat. 2016, 100, 32−46. DOI:10.1016/j.porgcoat.2016.02.022.
18. Bonardi, A.H.; Dumur F.; Grant, T.M.; Noirbent, G.; Gigmes, D.;Lessared, B.H.; Foussier, J. P.; Lelevee, J.. High performance near-Infrared (NIR) photoinitiating systems operating under low light intensity and in the presence of oxygen. Macromolecules, 2018, 51, 1314-1324. DOI: 10.1021/acs.macromol.8b00051.
19. Lin J.T.; Liu HW,; Chen KT,; Chiu YC, ; Cheng DC. Enhancing UV photopolymerization by a red-light pre-irradiation: kinetics and modeling strategies for reduced oxygen-inhibition. J Polym Sci, 2020，58， 683-691，DOI:10.1002/pol.20190201.
20. Lin J.T.; Chen K.T.; Cheng D.C.; Liu, H,W. Dual-wavelength (UV and Blue) controlled photopolymerization confinement for 3D-printing: modeling and analysis of measurements. Polymers, 2019, 11, 1819. DOI: 10.3390/polym11111819.
21. Lin, J.T.; Liu, H.W.; Chen, K.T.; Cheng, D..C. 3-wavelength (UV, blue, red) controlled photopolymerization: improved conversion and confinement in 3D-printing. IEEE Access, 2020, 8, 49353-49362. **DOI:** 10.1109/ACCESS.2020.2979172.
22. Liu, S.; Chen, H.; Zhang, Y.; Sun, K.; Xu, Y.; Motiet-Savary, F.; Graff, B.; Noirbent, G. Pigot, C.; Brunel, D. Lalevee, J. Monocomponent photoinitiators based on Benzophenone-carbazole structure for LED photoinitiating systems and application on 3D printing. Polymers, 2020, *12*, 1394. https://doi.org/10.3390/polym12061394.
23. Abdallah, M..; Hijazi,A.; Lin, J.T.; Graff, B.; Dumur, F.; Lalevee, J. Coumarin Derivatives as Photoinitiators in Photo-Oxidation and Photo-Reduction Processes and a Kinetic Model for Simulations of the Associated Polymerization Profiles. App Polym Mat. 2020, 2, 2769-2780. https://doi.org/10.1021/acsapm.0c00340.
24. Lin, J.T,; Lalevee, L.; Cheng. D,C. A Critical Review for Synergic Kinetics and Strategies for Enhanced Photopolymerizations for 3D-Printing and Additive Manufacturing. Polymers 2021, 13, 2325. https://doi.org/10.3390/polym13142325.
25. Lin, J.T. Efficacy S-formula and kinetics of oxygen-mediated (type-II) and non-oxygen-mediated (type-I) corneal cross-linking. Ophthalmology Research. 2018; 8(1): 1-11. DOI: 10.9734/OR/2018/39089 .
26. Lin, J.T.; Chen, K.T,; Cheng, D.C.; Liu, H.W. Modeling the efficacy of radical-mediated photopolymerization: the role of oxygen inhibition, viscosity and induction time. Front. Chem. 2019, 7:760. doi: 10.3389/fchem.2019.00760.

APPENDIX

Derivation of kinetic equations

The kinetic equations for our previous 2-initiator and 1-monomer system [24-26] were revised here for the 3-initiator and 2-monomer system, A/B/C/M/M', based on the schematic mechanisms of Eqs. (r1) to (r6) of Scheme 1 shown in the main text as follows. Also refer to the definitions shown in Fig. 1.

$$\frac{\partial[A]}{\partial t} = -bI(z,t)[A] + RGE \qquad (A1)$$

$$\frac{\partial[B]}{\partial t} = -(k_2T + k_7S')[B] \qquad (A2)$$

$$\frac{\partial[C]}{\partial t} = -(k_3T + k_6R")[C] \qquad (A3)$$

$$\frac{\partial T}{\partial t} = bI(z,t)[A] - (k_5 + k_1[A] + k_2[B] + k_3[C] + kM)T \qquad (A4)$$

$$\frac{\partial R}{\partial t} = (k_1[A] + k_2[B])T - (kR + k"S + k'M)R \qquad (A5)$$

$$\frac{\partial R"}{\partial t} = k_2[B]T - k_6R"[C] \qquad (A6)$$

$$\frac{\partial S}{\partial t} = k_3T[C] + k_6R"[C] - KSM - k"RS \qquad (A7)$$

$$\frac{\partial S'}{\partial t} = k_3T[C] - k_7[B]S' - K'S'M' \qquad (A8)$$

where RGE = $k_5T+k_6R"[C]+k_7S'[B]+kM$, is the regeneration term of of [A]. $b=83.6a'wq$, where w is the UV light wavelength (in cm) and q is the triplet state, T, quantum yield; a' is the mole absorption coefficient, in (1/mM/%) and I (z, t) is the light intensity, in mW/cm^2. Greater details of the rate constants were defined previously in Ref. [26] and they are related by the coupling terms. For examples, k_j (with j=1,2,3) are for the couplings of T and [A], [B], and [C], respectively; k_6 and k_7 are for the couplings of R and [C], and S′ and [B],

Preprints (www.preprints.org) | NOT PEER-REVIEWED | Posted: 2 June 2022 doi:10.20944/preprints202107.0327.v2

respectively; and k_T is the bimolecular termination rate of S. The couplings among T, R, S, and S and M (M′) for polymerization are given by k_8, k_{89}, K and K′, respectively.

The monomers conversions for FRP and CP, given by M and M', resepctively, may be obtained by the following equations [23]

$$\frac{dM}{dt} = -(kT + KS + k'R)M \qquad (A9)$$

$$\frac{dM'}{dt} = -K'S'M' \qquad (A10)$$

which are governed by the interaction of (T,R,S) and M; and S′ and M′, respectively.

We note that Eq. (A1) to (A10) are constructed for the specific system of Liu et al. [22], in which the following couplings (or effects) were ignored: oxygen inhibition, couplings of S and S′, R and S, R and [B], R and [A], S′ and [A] and the direct coupling of initiators, [A], [B], [C] and the monomers, M and M′ (type-I processes). For [A] alone, we assumed the FRP is mainly due to T and R, and the coupling of R′ and M was ignored here. We also limited here the FRP is dominated by the bimolecular termination of S, whereas CP is dominated by the unimolecular termination of S′. We have also reported results for more complex systems, including the above couplings and the oxygen inhibition effects [26].

For comprehensive modeling we will use the so-called quasi-steady state assumption [15, 18]. The life time of the singlet and triplet states of photosensitizer, and the radicals (R, S and S′) are very short, since they either decay or react with cellular matrix immediately after they are created. Thus, one may set dT/dt=dR/dt=dS′/dt=dR"/dt=0, which give the quasi-steady-state solutions: T=bIg[A], S′= k_3[C]Tg' and S= (k_3[C]+k_2[B])Tg"; with g=1/(k_5+k_1[A]+k_2[B]+k_3[C]+kM), g′=1/(k_7[B]+K'M') and g"=1 /(k"R+KM). Under these quasi-steady-state conditions, RGE =T/g- k_1[A]T= bI[A]- k_1[A]T, and d[A]/dt = - (Ib[A]-RGE)= - k_1[A]T. The approximated solution is given by [A]=A_0 exp[-X(t)], where X(t) is the time integral of k_1T(t). Therefore, when k_1=0, or there is a very weak type-I coupling with type-II dominant, d[A]/dt=0, which defines a perfect regeneration, or [A]=A_0 is a constant.

The steady state solution of Eq. (A7) is more complex, and is given by the solution of

$$k'R^2 + GR - P = 0 \qquad (A11)$$

where G=k"S+k'M, and P= (k_1[A]+k_2[B])T. Solving for R, we obtain

$$R = \left(\frac{1}{2k'}\right)(-G + \sqrt{G^2 + 4k'H}) \qquad (A12)$$

Analytic formulas of R can be obtained for two special cases.

Case (i) for dominant unimolecular termination, or G>>k'P, we obtain R= P/G, which is a linear increasing function of (k_1[A]+k_2[B])T/(k"S+k'M).

Case (ii) for dominant bimolecular termination, with P>> GR, we obtain, R=[P/k']$^{0.5}$, a nonlinear function of [(k_1[A]+k_2[B])T/k']$^{0.5}$, a square root function.

For analytic formulas we will consider a perfect catalytic cycle of the initiator, i.e., when G"=0, d[A]/dt=0, or [A]=A_0, is a constant. Also, for the case that g=1/(kM), g'=1/(K'M') and g"=1/(KM), for [B]<<K'M', or [B]=0), such that S'= k_3[C]T'/(kK'MM') and S= (k_3[C]+k_2[B])T'/(kKM^2), with T'=bIA_0. Using the first order solutions of M=M_0, and M'=M'$_0$ and [C]=C_0 exp(-dt), with d= k_3T'/(kM_0), we obtain the first-order solution [B]=B_0 exp(-d't), with d'= k_2T'/(kM_0)+ k_7k_3T'[C_0/(kM_0K'M'$_0$)]H(t), with H(t)=[1- exp(-dt)]/d, which allows us to find R, and solve for the efficacy of FRP and CP from Eq. (A9) and (A10) as follows.

The time integral of K'S' in Eq. (A10) leads to the solution fo CP, M'(t)= M$_0$' - K'D(bIC_0A_0)H(t), with H(t)=[1- exp(-dt)]/d, and D= k_7k_3[C_0/(kM_0K'M'$_0$). Therefore, the CE of CP is given by CE'=1-M/M_0 , or

$$CE' = K'D(bIC_0A_0)H(t), \qquad (A13)$$

which has a transient state proportional to bIt, but a steady state given by CE'=K'D(bIC_0A_0)/d= K'D(C_0A_0)[k_3/(kM_0)], which is independent of the light intensity (I). (A13) is for the case that g′=1/(k_7[B]+K'M')=1/(K'M'), when [B]=0. The second-order

 doi:10.20944/preprints202107.0327.v2

solution of S' , in the presence of [B], leads to a revised formula CE''= [1- $k_7B_0/(K'M_0')$] CE', with a reduction factor F'=1- $k_7B_0/(K'M_0')$. This fomula is based on a perfect regeneration case. If we include the second-oder solution [A]=A_0 exp[-X't], where X' is the time average of X(t), Eq. (A13) needs a revised H(t)=[1- exp(-d't)]/d', with a revised d'=d+X'.

Similarly, the time integral of K'S' in Eq. (A9) leads to the solution for FRP given by

$$CE= (T'/M_0)t+KD'H(t)+ KD''H'(t) + P'H''(t) , \quad (A14)$$

with H'(t)=[1- exp(-d't)]/d' ; D'= $k_3(C_0/Q)T'$, D''= $k_2(B_0/Q)$, with Q=$(kK'M'_0)$. And H''(t) depends on the solutions of R given by Eq. (A12) as follows. For case (i) R= [$(k_1[A]+k_2[B])T/(k'M)$[1- k''S/$(k'M_0)$], we obtain H''(t)= Pt+P'H'''(t), with H'''=[1- exp(d''t)]/d'', with P= $k_1(A_0^2/M_0)T'$, , P'=$k_2(B_0/M_0)T'$, and d''= [$k_2T'/(kM_0)$+ $0.5k_7k_3T't[C_0/(kM_0K'M'_0)$]t. For case (ii) k'R=[$k'(k_1[A]+k_2[B])T]^{0.5}$, we obtain H''(t)= Vt+V'H'''(t), with V= $(k_1 (A_0M_0)T')^{0.5}$, , V'=$(k_2 (B_0M_0)T')^{0.5}$. We note that all all the 4 terms in Eq. (A14) have transient state proportional to T't (or bItA_0). In comparison, the steady state of H(t)=1/d', H'''(t)=1/d'', which are independent to the light intensity (I). Similar to the CP case, we may include the second-oder solution [A]=A_0 exp[-X't], with X' is the time average of X(t), then Eq. (A16) needs a revision factor such that T' is revised to T''=T'[1- exp(-X't)]/X', which has a steady state solution independent of the light intensity (I).